Effects of Image Segmentation for Approximating Object Appearance Under Near Lighting

Takahiro Okabe and Yoichi Sato

Institute of Industrial Science, The University of Tokyo,
4-6-1 Komaba, Meguro-ku, Tokyo 153-8505, Japan
{takahiro, ysato}@iis.u-tokyo.ac.jp

Abstract. Shading analysis of an object under near lighting is not an easy task, because the direction and distance of the light source vary over the surface of the object. Observing a small area on the surface, however, techniques assuming far lighting are applicable, because variations of the direction and distance are small in the area. In this paper, we present two contributions to image segmentation for approximating object's appearance under near light sources. First, we experimentally evaluate the accuracy of approximations using rectangular segmentation for images of objects under near light sources, and confirm the effects of image segmentation itself. Second, we propose a novel segmentation method for approximating images under near light sources. Our proposed method plans appropriate segmentations in terms of approximation accuracy, considering properties of objects and variable illumination conditions.

1 Introduction

The effect of illumination on the appearance of objects is one of the most important research topics in computer vision. For the last decade, analysis of object's appearance under *far lighting* has made great progress.

For instance, Shashua [22] represented images of a Lambertian object under directional light sources by using three basis images of the object. Belhumeur and Kriegman [4] proved that a set of images of a convex Lambertian object under arbitrary directional light sources forms the illumination cone which is constructed from as few as three images of the object. Ramamoorthi-Hanrahan [17] and Basri-Jacobs [2] theoretically showed that the illumination cone can be approximately represented by linear combinations of 4 to 9 basis images. Based on these analyses assuming far lighting, a number of methods have been proposed for problems such as face recognition [10, 2, 5, 15], shape from motion [24, 7], forward rendering [19, 25, 21], and inverse rendering [18, 14].

To take one step further, we think that now is a good time for reconsidering the effects of *near lighting* on object's appearance. Let us consider an object with a size s illuminated by a point light source from a distance d. When the distance between the light source and the object is much larger than the size

P.J. Narayanan et al. (Eds.): ACCV 2006, LNCS 3851, pp. 764–775, 2006.

of the object ($s \ll d$), we can consider the light source as far lighting, that is, a directional light source. On the other hand, when the distance is less than or comparable to the size ($s > d$ or $s \sim d$), the light source should be treated as near lighting. It is well known that the analysis of object's appearance under near lighting is difficult because the direction and distance of the light source vary over the surface of the object.

The basic idea of our study is that, by segmenting an image of an object under near lighting, we can treat the image as if it were taken under far lighting. In other words, observing a small domain on the object surface, the domain size $\triangle s$ can become much smaller than the light source distance ($\triangle s \ll d$), even though the object size is larger than the distance. Therefore, techniques assuming far lighting are applicable to each domain on the object's surface.

Obviously, the assumption of directional lighting becomes more accurate as the number of domains increases. However, in practice, it is not appropriate to merely increase the number of domains for applying techniques assuming directional lighting. In the context of forward rendering [25], for example, more computing time is required as the number of domains increases. The performance of face recognition based on linear subspaces [10, 2] would get worse as the number of domains increases, because reconstruction errors due to false identity are also decreased. In addition, inverse rendering such as estimation of illumination [13] becomes ill-conditioned, as each domain gets close to an infinitesimal flat surface.

Accordingly, we discuss how to segment images of an object for applying techniques assuming directional lighting. More specifically, we propose a new segmentation method for approximating images under near light sources, in analogy with principal component analysis (PCA) that is optimal in the sense of approximation. Our proposed method finds the optimal segmentation in terms of approximation accuracy based on the difference between appearance under near lighting and that under far lighting, provided that the number of domains is given. In particular, our method enables us to plan appropriate segmentations considering properties of objects and variable illumination conditions.

The main contributions of our study are summarized as follows. First, we experimentally evaluate the accuracy of approximations using rectangular segmentation, and confirm the effects of image segmentation itself. As far as we know, no study has been done even on the effects of simple rectangular segmentation for dealing with the appearance of objects under near light sources. Second, we propose a new segmentation method for approximating images under near lighting. To demonstrate the effectiveness of our proposed method, we conducted a number of experiments by using synthetic and real images.

2 Related Work

The effect of near lighting has been studied in the both fields of image analysis and image synthesis. In the field of computer graphics, the effect of near lighting on the appearance of objects is often represented by interpolation [25] or extrapolation [1]. For example, Sloan *et al.* [25] compute angular distributions of illumination at some points on an object's surface in terms of spherical harmonics coefficients, and interpolate them over the surface.

In the field of computer vision, two different approaches are possible for the analysis of object appearance under near lighting: a *direct approach* and an *indirect approach.*

Direct Approach

The brightness of a point on an object's surface under a near point light source is represented by a nonlinear function with respect to the depth of the point and the position of the light source. We call the approach that explicitly solves the nonlinear equation relating the brightness with the depth and the light source position the direct approach. This approach has been studied for a long time, focusing mainly on how to stably solve nonlinear equations.

Iwahori *et al.* [11] proposed a method for acquiring the surface normal and depth of a Lambertian object from images of the object taken under a controlled point light source. Then, Kim and Burger [12] investigated the relationship between arrangement of the light sources and uniqueness of the solution of the nonlinear equations. Furthermore, Clark [6] extended photometric stereo under near point light sources to that under a moving point light source.

Thus, the direct approach has achieved important progress in modeling objects. However, it is not trivial to extend these methods to deal with complex light sources, because they assume simple illumination conditions such as a single point light source.

Indirect Approach

In contrast to the direct approach, the indirect approach does not deal with the nonlinear function explicitly, but approximately represents object's appearance under near lighting. As described in Section 1, image segmentation is one of the feasible ways for approximating images under near lighting.

The idea of image segmentation is not necessarily new for object recognition. Zhao and Yang [26, 27] proposed the mosaic image method in the context of PCA with outliers such as occlusions, specular highlights, and shadows. The method segments an image into rectangular blocks and applies PCA to each block. They described that the assumption of directional lighting becomes more accurate by segmenting images. However, effects of image segmentation on object's appearance under near lighting were not examined.

Image segmentation is applied also to face recognition under varying illumination conditions. Batur and Hayes [3] divided an image into a set of small images with similar surface normals, and applied the linear subspace method [22] to each small image. Sakaue and Shakunaga [20] also combined rectangular segmentation with PCA-based face recognition. However, the main purpose of these studies was to achieve robust face recognition against shadows under directional light sources. Therefore, effects of near light sources were not examined.

Another way for approximating images under near light sources was recently proposed by Frolova *et al.* [9]. It is well known that images of a Lambertian object under directional light sources are approximately represented by using low-frequency terms of spherical harmonics [17, 2]. The point of the study is to represent effects of near lighting by using high-frequency terms of spherical harmonics. It is reported that the method using high-frequency terms works well for images of a sphere. However, the method is not applicable to objects such as a plane, because the basis images depend only on surface normals.

3 Proposed Method

3.1 Overview

We consider a set of images of a static object taken from a fixed viewpoint under variable illumination conditions. We assume that the shape and reflectance properties of the object and the statistical properties of the variable illumination are known. For simplicity, we assume that an illumination distribution is represented by a set of point light sources[1].

Let us segment the surface of an object into c domains and consider points on the object surface that belong to one of the domains. When a point p on the object surface belongs to the i-th domain D_i whose center is a point P_i, we denote the approximation error at the point p by $\mathrm{err}(p, P_i)$. Our proposed method minimizes the objective function J described by

$$J = \sum_{i=1}^{c} \sum_{p \in D_i} \mathrm{err}(p, P_i), \tag{1}$$

in order to find the optimal segmentation in terms of approximation accuracy[2].

In Section 3.2, we define the error function $\mathrm{err}(p, P_i)$ of a scene where an object is illuminated by a single point light source. In Section 3.3, we extend the error function to the scene under complex and variable illumination distributions. Finally, in Section 3.4, we describe the detailed algorithm of our method based on k-means clustering [8].

3.2 Criterion I: Single Point Light Source

Let us consider an object illuminated by a single point light source with unit radiance, and denote the positions of the point p, the center P_i, and the light source by $\boldsymbol{x}$, $\boldsymbol{X}$, and $\boldsymbol{R}$ respectively (Fig. 1). Assuming the Lambertian model[3], the brightness I at the point p is represented by

$$I = \rho \boldsymbol{n} \cdot (\boldsymbol{R} - \boldsymbol{x}) S_{\boldsymbol{n}, \boldsymbol{R}-\boldsymbol{x}} / |\boldsymbol{R} - \boldsymbol{x}|^3, \tag{2}$$

where ρ and $\boldsymbol{n}$ are the albedo and surface normal at the point. The coefficient $S_{\boldsymbol{n}, \boldsymbol{R}-\boldsymbol{x}}$ represents both attached and cast shadows. Namely, $S_{\boldsymbol{n}, \boldsymbol{R}-\boldsymbol{x}} = 0$ if

---

[1] Here, we assume isotropic lighting. Thus, we do not take account of anisotropic light sources such as a projector.

[2] Because our objective is to approximate images, we sum up the approximation errors not over the surface of an object but over the image plane.

[3] We can extend the following discussion to other reflectance models except for mirror-like reflectance.

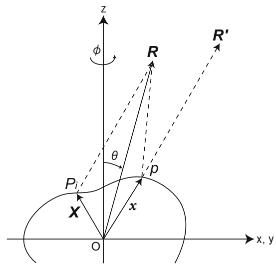

Fig. 1. Coordinate system

$\boldsymbol{n} \cdot (\boldsymbol{R} - \boldsymbol{x}) < 0$ or the direction of the light source $(\boldsymbol{R} - \boldsymbol{x})$ is occluded by the object, and $S_{\boldsymbol{n},\boldsymbol{R}-\boldsymbol{x}} = 1$ otherwise.

If the assumption of far lighting is accurate over the domain, the brightness of the point p is nearly constant when the position of the light source seen from the point p, that is, $(\boldsymbol{R} - \boldsymbol{x})$ is replaced by that seen from the center of the domain P_i, that is, $(\boldsymbol{R} - \boldsymbol{X})$. In other words, we can consider the point p as if it were illuminated by a point light source located at $\boldsymbol{R}' = \boldsymbol{x} + (\boldsymbol{R} - \boldsymbol{X})$. Thus, we consider I' defined by

$$I' = \rho \boldsymbol{n} \cdot (\boldsymbol{R} - \boldsymbol{X}) S_{\boldsymbol{n},\boldsymbol{R}-\boldsymbol{X}} / |\boldsymbol{R} - \boldsymbol{X}|^3 \tag{3}$$

as the brightness at the point p under the assumption of directional lighting, and define the error function as

$$\mathrm{err}(p, P_i) = (I - I')^2. \tag{4}$$

3.3 Criterion II: General Illumination Condition

Our objective is to minimize the approximation error of a set of images taken under variable illumination conditions. Let $L(\boldsymbol{r})$ denote the average illumination radiance at each 3D point $\boldsymbol{r}$ in a scene, which is the average with respect to the variable illumination conditions. Then, we can simply extend the error function in equation (4) to that under the variable illumination conditions, by summing up $(I - I')^2$ for each point light source with the weight corresponding to the average distribution $L(\boldsymbol{r})$ of the variable illumination. Replacing the summation by an integral, the error functions of an object illuminated by light sources at the distance $|\boldsymbol{R}| = R$, for example, are represented by integrals such as $\int_0^{2\pi} \int_0^{\pi} (I - I')^2 L(R, \theta, \phi) \sin\theta d\theta d\phi$. Here, $L(R, \theta, \phi)$ is the average distribution of illumination represented by the spherical coordinates. In the same way, we can take into account variations of distances from the object to light sources.

However, the above extension is not practical in terms of computational cost. In the segmentation algorithm described later, we have to calculate the above integrals for each iteration step, or compute them in advance. In the latter case, because the integrands depend both on the point p and on the domain center P_i, we have to precompute them for all combinations of pixels. Then, the number of integrations required becomes $O(N^2)$ for an image with N pixels. Therefore, this simple extension requires a large amount of computing time or storage.

Accordingly, taking the Taylor series expansion of $(I - I')$ under the conditions that $|\boldsymbol{R}| > |\boldsymbol{x}|$ and $|\boldsymbol{R}| > |\boldsymbol{X}|$, we focus on the first order effect represented by

$$I - I' \simeq (\rho/R^3)[(3\boldsymbol{R}\cdot\boldsymbol{n}/R^2)\boldsymbol{R} - \boldsymbol{n}]\cdot(\boldsymbol{x} - \boldsymbol{X})S_{\boldsymbol{n},\boldsymbol{R}}, \tag{5}$$

when the assumption of far lighting begins to break down. As a result, the error function is represented as

$$\mathrm{err}(p, P_i) = \textstyle\sum_{j=1}^{3}\sum_{k=1}^{3} g_{jk}(x_j - X_j)(x_k - X_k). \tag{6}$$

This means that we should calculate the error, that is, "distance" between the point p and the center P_i with the "metrics" g_{jk} defined by

$$g_{jk} \equiv \frac{\rho^2}{R^6}\int_0^{2\pi}\int_0^{\pi}\left(\frac{3\boldsymbol{R}\cdot\boldsymbol{n}}{R^2}R_j - n_j\right)\left(\frac{3\boldsymbol{R}\cdot\boldsymbol{n}}{R^2}R_k - n_k\right)S_{\boldsymbol{n},\boldsymbol{R}}L(R,\theta,\phi)\sin\theta d\theta d\phi, \tag{7}$$

based on properties of the object and illumination, instead of the Euclidean metrics ($g_{jk} = \delta_{jk}$). The approximation in equation (5) makes our method more tractable. We can numerically precompute $O(N)$ metrics[4], because the integrand in equation (7) is independent of the domain center P_i and depends only on the point p.

3.4 Segmentation Method

Our proposed method finds the image segmentation that minimizes the objective function J in equation (1). Basically, we give initial positions of domain centers. Then, we assign a point p to the domain that minimizes $\mathrm{err}(p, P_i)$ with respect to P_i, and update the center of domain $P_i'(\in D_i)$ so that $\sum_{p\in D_i}\mathrm{err}(p, P_i')$ is minimized. The last two steps are repeated until the segmentation converges.

In order to alleviate the problem of local minima, we take a coarse-to-fine approach. Actually, we repeat the above steps and update the temporary optimal positions of domain centers if the i-th value of the objective function J_i is minimal at the time. For the coarse search of the minimum, initial positions of centers are randomly sampled in the first N_{sample} iterations. On the other hand, in the last N_{resample} iterations, we resample these positions around the temporary optimal positions for the fine search[5].

---

[4] We computed the integrals by using Gaussian quadratures [16] assuming that the bandwidth of the integrands equals 50. Thus, we sampled the integrands at about 5000 directions.

[5] We set $N_{\mathrm{sample}} = 1000$ and N_{resample}=9000, based on preliminary experiments.

4 Experiments

4.1 Qualitative Properties

To begin with, we describe qualitative properties of the image segmentation obtained by using our proposed method.

We considered a part of a Lambertian sphere with uniform albedo as a target object (Fig. 2 (a)), and planned appropriate segmentations for three different average distributions of illumination. Let (r, θ, ϕ) be the spherical coordinates whose center $(r = 0)$ and north pole $(\theta = 0)$ are the center of the sphere and the direction of the z axis (the line of sight) respectively. The first condition corresponds to a point light source located at $(r, \theta, \phi) = (2r_s, \pi/4, 3\pi/4)$. Here, r_s is the radius of the sphere. The second one corresponds to a point light source that distributes at $\Omega = \{(\theta, \phi) | \pi/6 \leq \theta \leq \pi/2, 0 \leq \phi \leq \pi/2\}$ with uniform probability density. The third one is $L(R, \theta, \phi) =$ const. in equation (7), that is, a point light source that uniformly distributes around the sphere.

We show segmentation results as gray images in Fig. 2. The first, second, and third conditions correspond to (b), (c), and (d). The number of domains is 9 (16) in the upper (lower) row. The gray value of a pixel is proportional to the number of pixels belonging to the same domain as the pixel does. Therefore, the darker a pixel is, the smaller domain the pixel belongs to. Portions of images are saturated, because we set the gray value of the domain with average pixel number $(= N/c)$ to 128.

This study shows three important properties as follows. (i) *Points in a domain are not necessarily close to each other in the sense of the Euclidean distance.* As mentioned in Section 3.3, the size of a domain changes according to the geometric and photometric properties of the scene. (ii) *The size of a domain becomes smaller as the domain comes close to light sources.* This property is consistent with our intuition. Variations of domain size are dominant when the average distribution of illumination is concentrated in a small solid angle as in results (b) and (c). (iii) *The size of a domain becomes smaller as variations of depth becomes larger in the domain.* As shown in results (d), this property is dominant when an average illumination distribution is isotropic. This shows that we should segment images of a scene based on the depth, even though we cannot obtain any prior knowledge about illumination as in the case of inverse lighting.

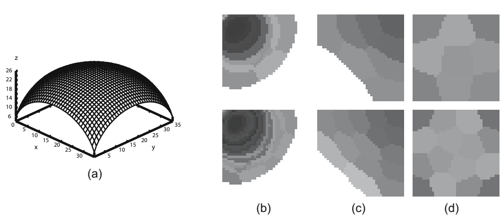

Fig. 2. (a) 3D shape of a target object and segmentation results of the object under (b) a point light source, (c) a set of point light sources with an area distribution, and (d) uniform illumination

4.2 Approximation Accuracy of Synthetic Images

Second, we conducted a number of experiments by using synthetic images so that we could rigorously evaluate the approximation accuracy. As described below, we reconstructed diffuse reflection components of the target object under point light sources by projecting input images to the basis images.

Let I_j be the brightness of a point p_j corresponding to the j-th pixel ($j = 1, 2, ..., N$), and $\boldsymbol{b}_j$ be the basis vector defined by

$$\boldsymbol{b}_j = \rho_j \boldsymbol{n}_j, \tag{8}$$

where ρ_j and $\boldsymbol{n}_j$ are the albedo and surface normal at the point. We calculated the coefficients $\boldsymbol{s}_i$ of the basis vectors in the i-th domain by minimizing $\sum_{p_j \in D_i} w_j (I_j - \boldsymbol{s}_i \cdot \boldsymbol{b}_j)^2$. Here, we set $w_j = 0$ if $I_j = 0$ and $w_j = 1$ otherwise so that shadows are removed. Then, we defined the reconstruction error as

$$\epsilon = \textstyle\sum_{i=1}^{c} \sum_{p_j \in D_i} w_j (I_j - \boldsymbol{s}_i \cdot \boldsymbol{b}_j)^2 / \sum_{j=1}^{N} I_j^2. \tag{9}$$

We tested three average distributions of illumination. The first and second conditions correspond to point light sources located at $(2r_s, \pi/4, 3\pi/4)$ and $(3r_s, \pi/4, 3\pi/4)$ respectively. The third one is a point light source uniformly distributed at $\Omega = \{(\theta, \phi) | \pi/6 \leq \theta \leq \pi/2, 0 \leq \phi \leq \pi/2\}$.

Under the first illumination condition, we synthesized an input image of the object and reconstructed it. In Fig. 3, we show (a) the input image and reconstructed images (b) without image segmentation, (c) by using rectangular segmentation with 16 domains, and (d) by using our proposed method with the same number of domains. The reconstruction error against the number of domains is shown in Fig. 4 (a). The solid and dotted lines represent the errors of rectangular segmentation and our method respectively. One can find that image segmentation drastically improves the approximation accuracy. In the case of rectangular segmentation with 36 domains, for example, the error decreases about 2 orders of magnitude. Furthermore, the error of our method is several factors smaller than that of rectangular segmentation. In other words, our method achieves higher approximation accuracy by using smaller number of domains. For the second illumination condition, we obtained a similar result (Fig. 4 (b)).

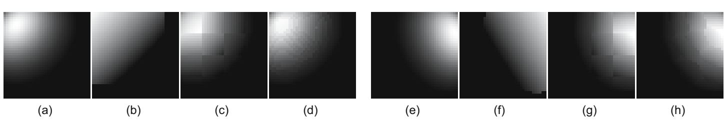

Fig. 3. Image reconstruction based on segmentation (sphere): (a) an input image under a point light source, reconstructed images (b) without segmentation, (c) with rectangular segmentation, and (d) with the segmentation obtained by using our method. Images (e) through (h) are those under another average distribution of illumination

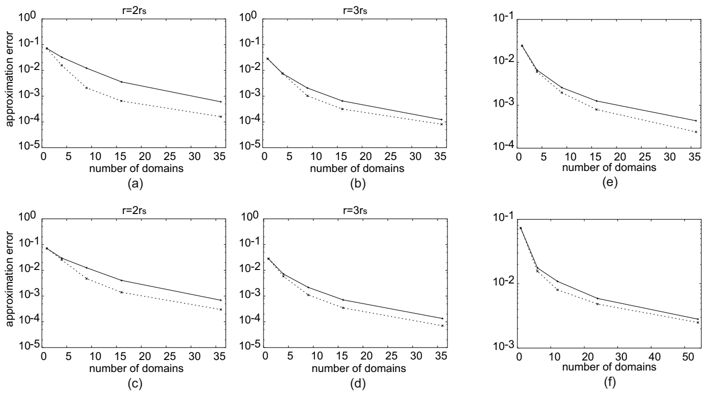

Fig. 4. Reconstruction errors of sphere images against the number of domains under a point light source located at (a) $2r_s$ or (b) $3r_s$, and under a set of point light sources located at (c) $2r_s$ or (d) $3r_s$. The solid and dotted lines represent the errors of rectangular segmentation and our method respectively. Reconstruction errors of images of a plaster sphere and those of a Napoleon figure are shown in (e) and (f).

For the third condition, we synthesized 100 images under point light sources located at a distance $2r_s$ or $3r_s$ and uniformly distributed within Ω, and reconstructed them (Fig. 3 (e), (f), (g), and (h)). The average reconstruction errors shown in Fig. 4 (c) and (d) behave in a similar manner to those under the first and second conditions.

4.3 Approximation Accuracy of Real Images

Third, we report the result of experiments using real images. In the experiments, various images of a plaster sphere were taken under far or near light sources by using SONY DXC-9000 camera and Matrox Meteor-II frame grabber. The distances between the center of the sphere and the far (near) light sources are more than 10 (about 2∼3) times the radius of the sphere.

We estimated three basis images of the sphere from 12 images taken under unknown far light sources by using singular value decomposition with missing data (SVDMD) [23]. We used 10 images taken under near light sources to confirm the effects of image segmentation for approximating the appearance. All images were cropped and down-sampled so that the geometry of the scene is the same as that in the experiments using synthetic images. The distribution of the near light sources roughly obeyed the third condition in the previous section.

In Fig. 4 (e), we show the average reconstruction error against the number of domains. One can find that the average reconstruction errors behave like those in Fig. 4 (a) through (d). Moreover, our method improves the approximation accuracy about 40% compared with rectangular segmentation. Hence, we can conclude that image segmentation, especially our proposed method, works well for approximating object's appearance under near light sources.

4.4 Discussion

Finally, we discuss the applicability of our proposed method to face recognition[6] under near light sources. More specifically, we conducted two experiments to confirm (i) whether segmentation results of different people resemble each other, and (ii) whether the image segmentation of the average face works well for other faces.

In the first experiment, we used the face database provided by the Max-Planck Institute for Biological Cybernetics [5]. This database contains laser-scanned face models of four persons and an average face model.

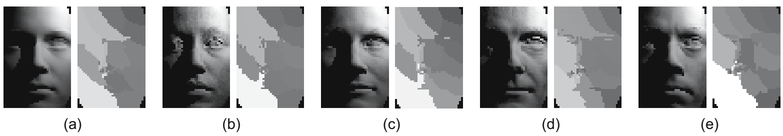

Fig. 5. Images and segmentation results of faces: (a) an average, and (b)∼(e) four persons

In Fig. 5, we show images under a typical point light source and segmentation results of (a) the average face and those of (b)∼(e) four persons. We assumed that the average distribution of illumination is uniform within $\Omega = \{(\theta, \phi) | \pi/6 \leq \theta \leq \pi/2, 0 \leq \phi \leq \pi/2\}$. One can see that these segmentation results resemble each other: pixels in the upper right and right regions belong to smaller domains than those in the lower left and left regions.

In the second experiment, we used images of a plaster Napoleon figure taken in a similar manner to that in Section 4.3. The average reconstruction error against the number of domains is shown in Fig. 4 (f). One can find that the average reconstruction errors behave in a similar manner to other results in Fig. 4. In spite of different geometry and deviations from our assumptions such as interreflections, our method improves the approximation accuracy about 20% compared with rectangular segmentation.

These experimental results imply that, for approximating face images under near lighting, we can substitute the segmentation result of the average face for those of individuals. Therefore, a combination of image segmentation for the average face and PCA-based face recognition *etc.* would be one of the feasible methods for face recognition under near light sources, even when 3D models of individuals are unavailable.

5 Conclusions and Future Work

In this paper, we discussed image segmentation in terms of approximation accuracy, which is a necessary condition for applying techniques assuming directional

[6] Strictly speaking, we investigate not recognition but approximation. However, the notion of Eigenfaces shows image approximation or compression is important also for face recognition.

light sources. In summary, the main contributions of the present study consist of (i) the experimental evaluation of image segmentation for dealing with object's appearance under near lighting, (ii) a method for planning appropriate segmentations considering properties of objects and variable illumination conditions.

In the future, we will extend our framework for image segmentation by considering sufficient conditions for specific applications such as face recognition and inverse rendering. Along with the compatibility with techniques assuming directional light sources, we believe that image segmentation is one of the most promising approaches to a number of applications dealing with images under near light sources.

Acknowledgements

A part of this work was supported by Grants-in-Aid for Scientific Research from the Ministry of Education, Culture, Sports, Science and Technology of Japan (No. 13224051).

References

1. T. Annen, J. Kautz, F. Durand, and H.-P. Seidel, "Spherical harmonic gradients for mid-range illumination", In *Proc. Eurographics Sympo. Rendering 2004*, pp.331–336, 2004.
2. R. Basri and D. Jacobs, "Lambertian reflectance and linear subspaces", *IEEE Trans. PAMI*, 25(2), pp.218–233, 2003.
3. A. Batur and M. Hayes, "Linear subspaces for illumination robust face recognition", In *Proc. IEEE CVPR 2001*, pp.II-296–301, 2001.
4. P. Belhumeur and D. Kriegman, "What is the set of images of an object under all possible lighting conditions?", *Int'l. J. Computer Vision*, 28(3), pp.245–260, 1998.
5. V. Blanz and T. Vetter, "Face recognition based on fitting a 3D morphable model", *IEEE Trans. PAMI*, 25(9), pp.1063–1074, 2003.
6. J. Clark, "Active photometric stereo", In *Proc. IEEE CVPR '92*, pp.29–34, 1992.
7. F. Du, T. Okabe, Y. Sato, and A. Sugimoto, "Reflectance estimation from motion under complex illumination", In *Proc. IAPR ICPR 2004*, pp.218–222, 2004.
8. R. Duda, P. Hart, and D. Stork, *Pattern Classification*, John Wiley & Sons, 2001.
9. D. Frolova, D. Simakov, and R. Basri, "Accuracy of spherical harmonics approximations for images of Lambertian objects under far and near lighting", In *Proc. ECCV 2004*, LNCS 3021, pp.574–587, 2004.
10. A. Georghiades, P. Belhumeur, and D. Kriegman, "From few to many: illumination cone models for face recognition under variable lighting and pose", *IEEE Trans. PAMI*, 23(6), pp.643–660, 2001.
11. Y. Iwahori, H. Sugie, and N. Ishii, "Reconstructing shape from shading images under point light source illumination", In *Proc. IEEE ICPR '90*, pp.I-83–87, 1990.
12. B. Kim and P. Burger, "Depth and shape from shading using the photometric stereo method", *CVGIP: Image Understanding*, 54(3), pp.416–427, 1991.
13. A. Marschner and D. Greenberg, "Inverse lighting for photography", In *Fifth Color Imaging Conference*, pp.262–265, 1997.

14. T. Okabe, I. Sato, and Y. Sato, "Spherical harmonics vs. Haar wavelets: basis for recovering illumination from cast shadows", In *Proc. IEEE CVPR 2004*, pp.I-50–57, 2004.
15. T. Okabe and Y. Sato, "Object recognition based on photometric alignment using RANSAC", In *Proc. IEEE CVPR 2003*, pp.I-221–228, 2003.
16. W. Press, S. Teukolsky, W. Vetterling, and B. Flannery, *Numerical Recipes in C*, Cambridge University Press, 1992.
17. R. Ramamoorthi and P. Hanrahan, "On the relationship between radiance and irradiance: determining the illumination from images of a convex Lambertian object", *J. Opt. Soc. Am. A*, 18(10), pp.2448–2459, 2001.
18. R. Ramamoorthi and P. Hanrahan, "A signal-processing framework for inverse rendering", In *Proc. ACM SIGGRAPH 2001*, pp.117–128, 2001.
19. R. Ramamoorthi and P. Hanrahan, "An efficient representation for irradiance environment maps", In *Proc. ACM SIGGRAPH 2001*, pp.497–500, 2001.
20. F. Sakaue and T. Shakunaga, "Face recognition by parallel partial projections", In *Proc. ACCV 2004*, pp.144–150, 2004.
21. I. Sato, T. Okabe, Y. Sato, and K. Ikeuchi, "Appearance sampling for obtaining a set of basis images for variable illumination", In *Proc. IEEE ICCV 2003*, pp.800–807, 2003.
22. A. Shashua, "On photometric issues in 3D visual recognition from a single 2D image", *Int'l. J. Computer Vision*, 21(1/2), pp.99–122, 1997.
23. H.-Y. Shum, K. Ikeuchi, and R. Reddy, "Principal component analysis with missing data and its application to polyhedral object modeling", *IEEE Trans. PAMI*, 17(9), pp.854–867, 1995.
24. D. Simakov, D. Frolova, and R. Basri, "Dense shape reconstruction of a moving object under arbitrary, unknown lighting", In *Proc. IEEE ICCV 2003*, pp.1202–1209, 2003.
25. P. Sloan, J. Kautz, and J. Snyder, "Precomputed radiance transfer for real-time rendering in dynamic, low frequency lighting environments", In *Proc. ACM SIGGRAPH 2002*, pp.527–536, 2002.
26. L. Zhao and Y.-H. Yang, "Theoretical analysis of illumination in PCA-based vision systems", *Pattern Recognition*, 32(4), pp.547–564, 1999.
27. L. Zhao and Y.-H. Yang, "Mosaic image method: a local and global method", *Pattern Recognition*, 32(8), pp.1421–1433, 1999.